Electronic Supplementary Information

Self-assembled ultrasmall mixed Co-W phosphide nanoparticles on pristine graphene with remarkable synergistic effects as highly efficient electroatalysts for hydrogen evolution

Xiaoyan Wang,[ab] Jia Bo Le,[c] Yang Fei,[d] Ruiqin Gao,[e] Maoxiang Jing,[f] Weiyong Yuan*[ag] and Chang Ming Li[h]

[a]Ningbo Research Institute, Zhejiang University, Ningbo 315100, China

[b]Research Center for Environmental and Energy Catalysis, Institute of Fundamental and Frontier Sciences, University of Electronic Science and Technology of China, Chengdu 611731, China.

[c]Ningbo Institute of Materials Technology and Engineering, Chinese Academy of Sciences, Ningbo 315201, China

[d]State Key Laboratory of Electronic Thin Film and Integrated Devices, School of Electronic Science and Engineering, University of Electronic Science and Technology of China, Chengdu 610054, China

[e]School of Biological and Chemical Engineering, NingboTech University, Ningbo 315100, China

[f]Institute for Advanced Materials, Jiangsu University, Zhenjiang 212013, China

[g]College of Chemical and Biological Engineering, Zhejiang University, Hangzhou 310027, China

[h]Institute of Materials Science and Devices, Suzhou University of Science and Technology, Suzhou 215009, China

*Corresponding author. E-mail: wyyuan@zju.edu.cn

Contents

HR) and TEM images of G@HPW (without HR) and G@HPW (Fig. S1).

2. EDX mapping of G@HPW after the hydrothermal reaction (Fig. S2).
3. High-resolution Co $2p_{3/2}$ and P 2p XPS spectra of the sample before phosphidation (Fig. S3).
4. Size distribution of Co-W-P NPs in G@Co-W-P (Fig. S4).
5. TEM and HRTEM images of Co-W-P/G and CoP/G (Fig. S5).
6. XRD patterns of one-step hydrothermal reaction and the sample with no HPW added in the second-step hydrothermal reaction (Fig. S6).
7. TEM image and high-resolution W 4f (B) and P 2p (C) XPS spectra of WP_2/G (Fig. S7).
8. Detailed comparison of the performance of G@W-Co-P in 0.5 M H_2SO_4 with those of representative non-noble-metal HER catalysts (Table S1).
9. Enlarged LSV curve of WP_2/G in 0.5 M H_2SO_4 (Fig. S8).
10. Detailed comparison of the performance of G@W-Co-P in 1 M KOH with those of representative non-noble-metal HER catalysts (Table S2).
11. XRD pattern of G@Co-W-P after the durability tests (Fig. S9).

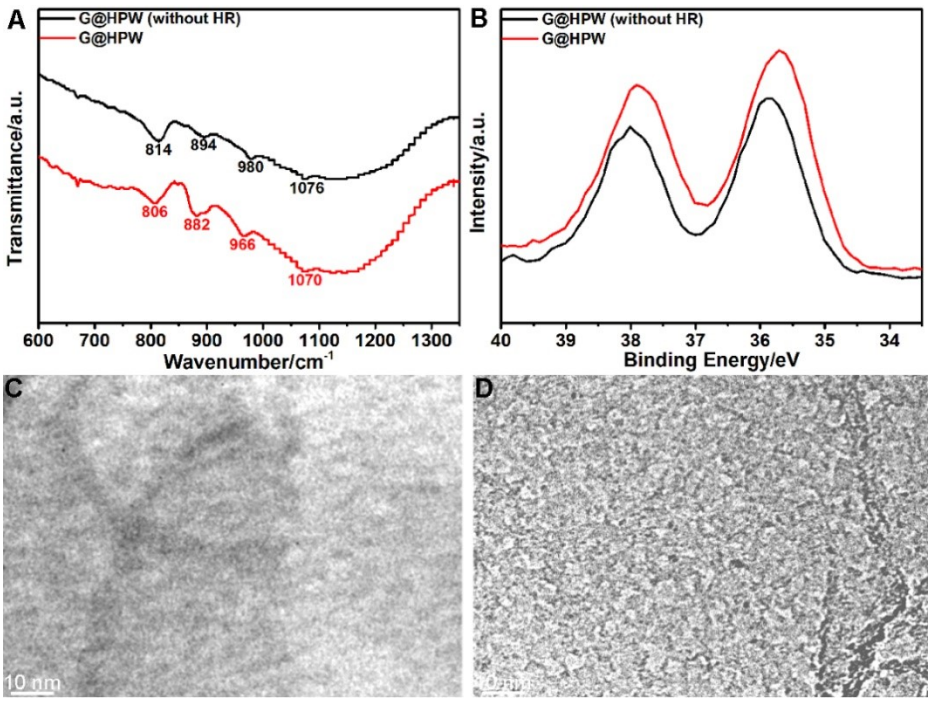

Fig. S1 FTIR spectra (**A**) and high-resolution W 4f XPS spectra (**B**) of G@HPW and G@HPW (without HR) and TEM images of G@HPW (without HR) (**C**) and G@HPW (**D**).

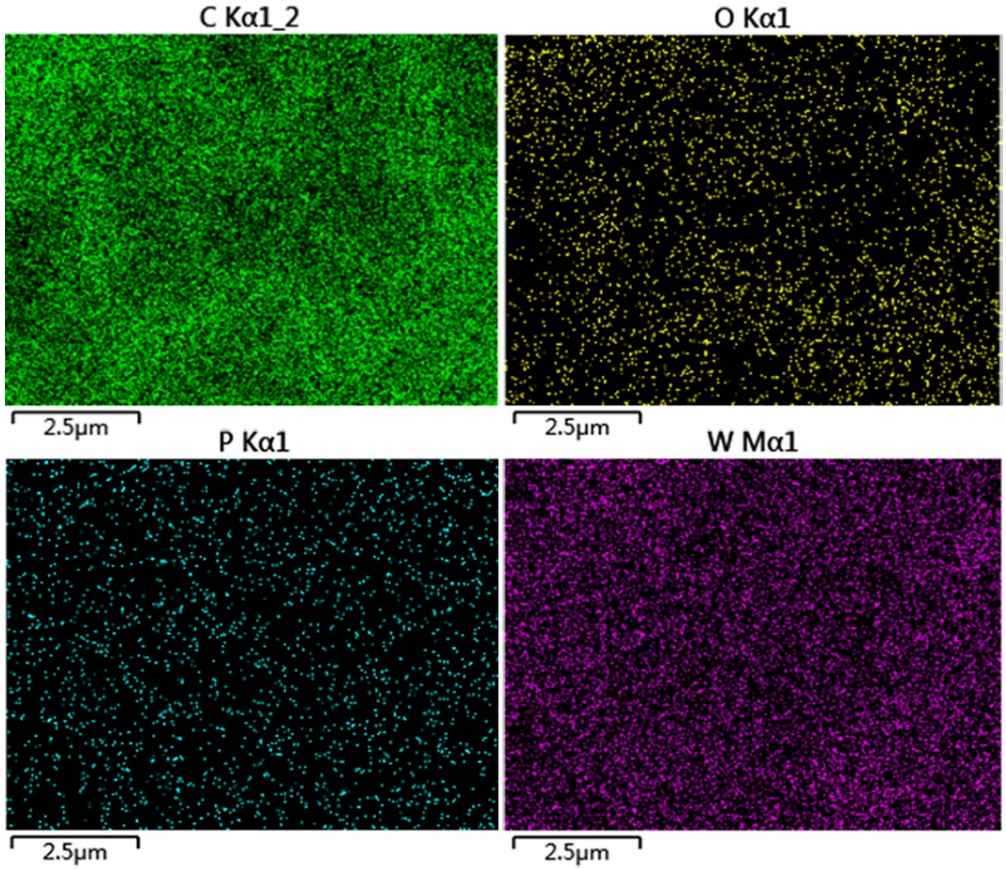

Fig. S2 EDX mapping of G@HPW after the hydrothermal reaction.

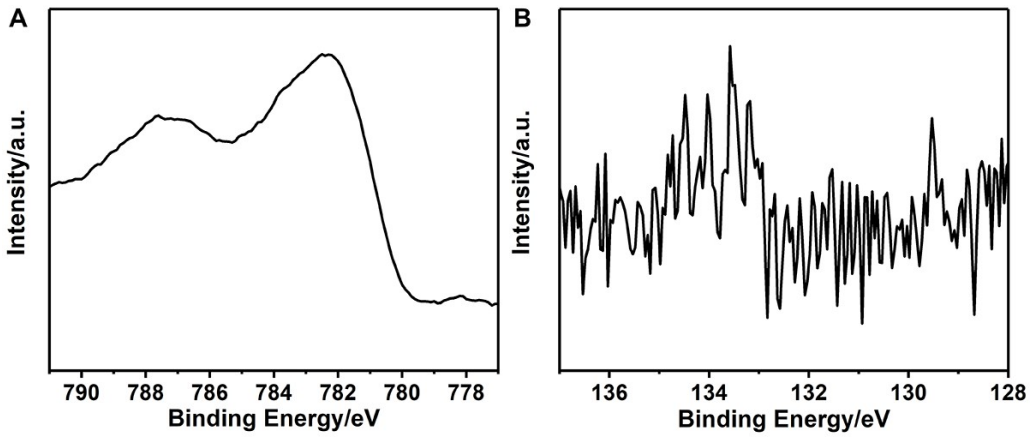

Fig. S3 High-resolution Co $2p_{3/2}$ (A) and P 2p (B) XPS spectra of the sample before phosphidation.

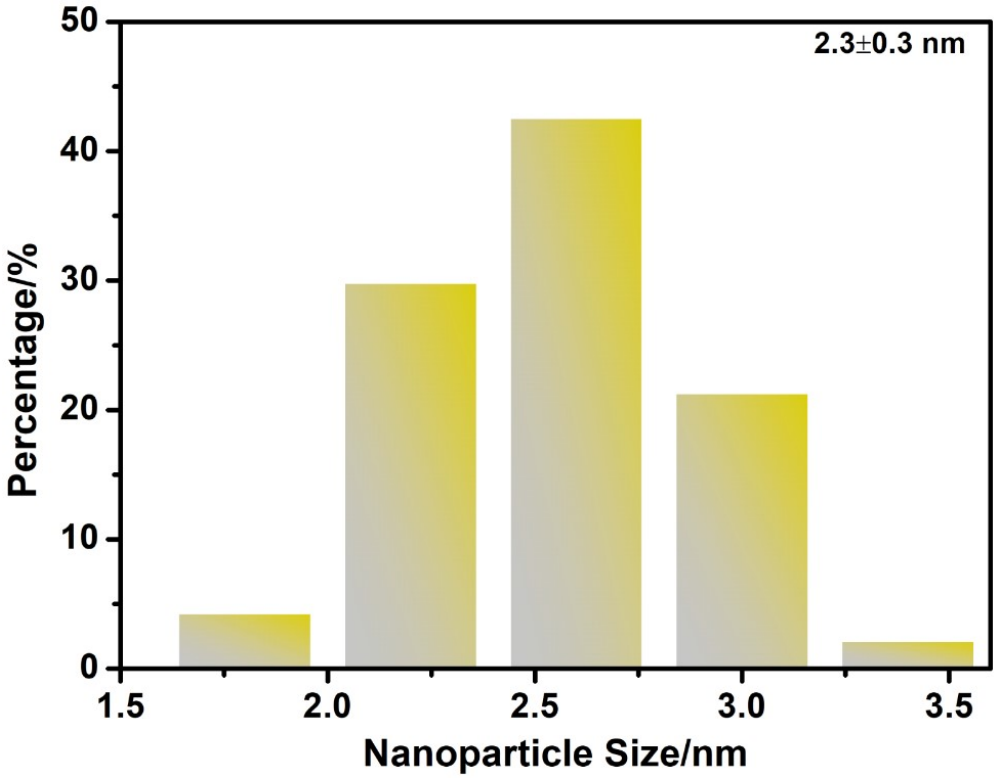

Fig. S4 Size distribution of Co-W-P NPs in G@Co-W-P.

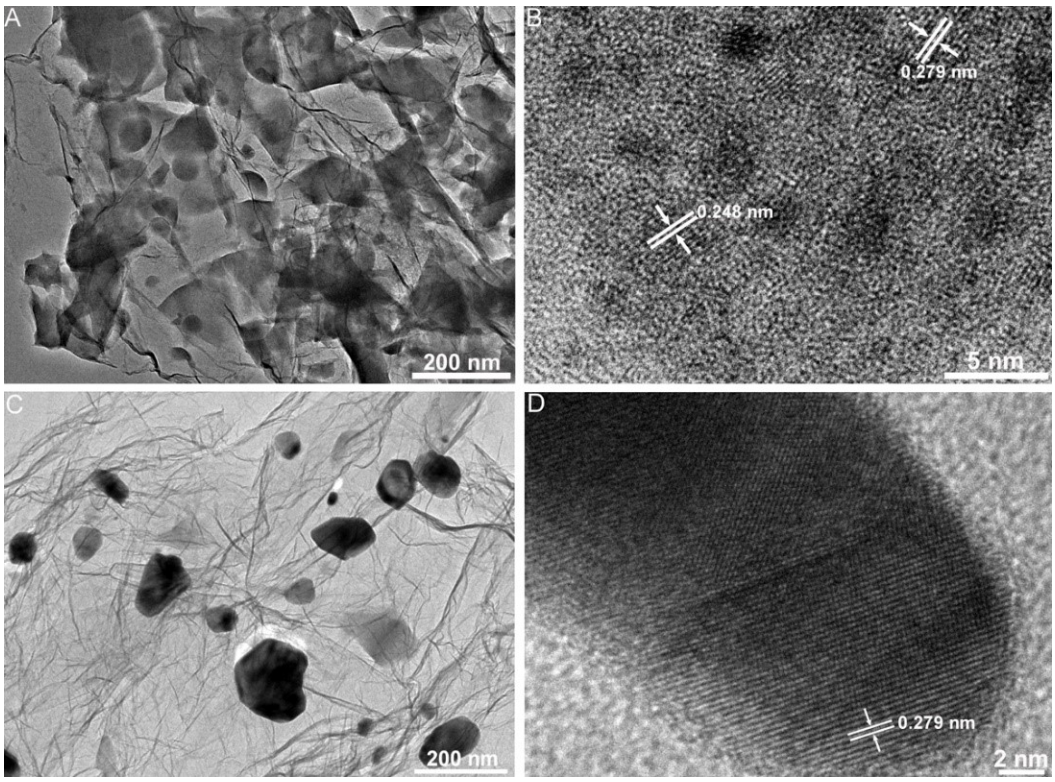

Fig. S5 TEM (**A** and **C**) and HRTEM (**B** and **D**) images of Co-W-P/G (**A** and **B**) and CoP/G (**C** and **D**).

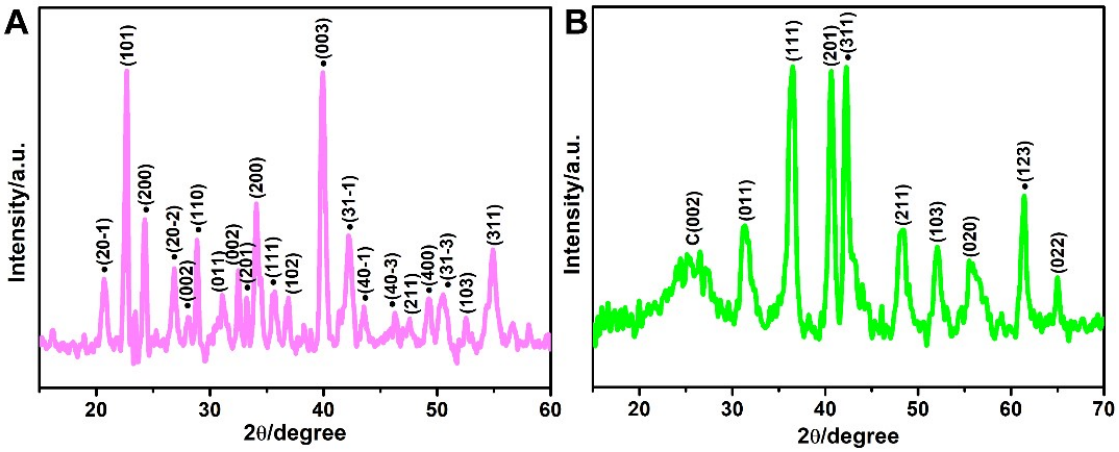

Fig. S6 XRD patterns of one-step hydrothermal reaction (**A**) and the sample with no HPW added in the second-step hydrothermal reaction (**B**). • above the XRD pattern in (**A**) represents characteristic peaks of WP_2 (JCPDS card no. 35-1467) and the other peaks are from CoP (JCPDS card no. 29-0497) (except the peak C (002), which is from graphene). There are some peaks from $Co_3(PO_4)_2$ (JCPDS card no. 77-0225) in (**B**) (labeled with •), which is formed due to the surface oxidation under high temperature.

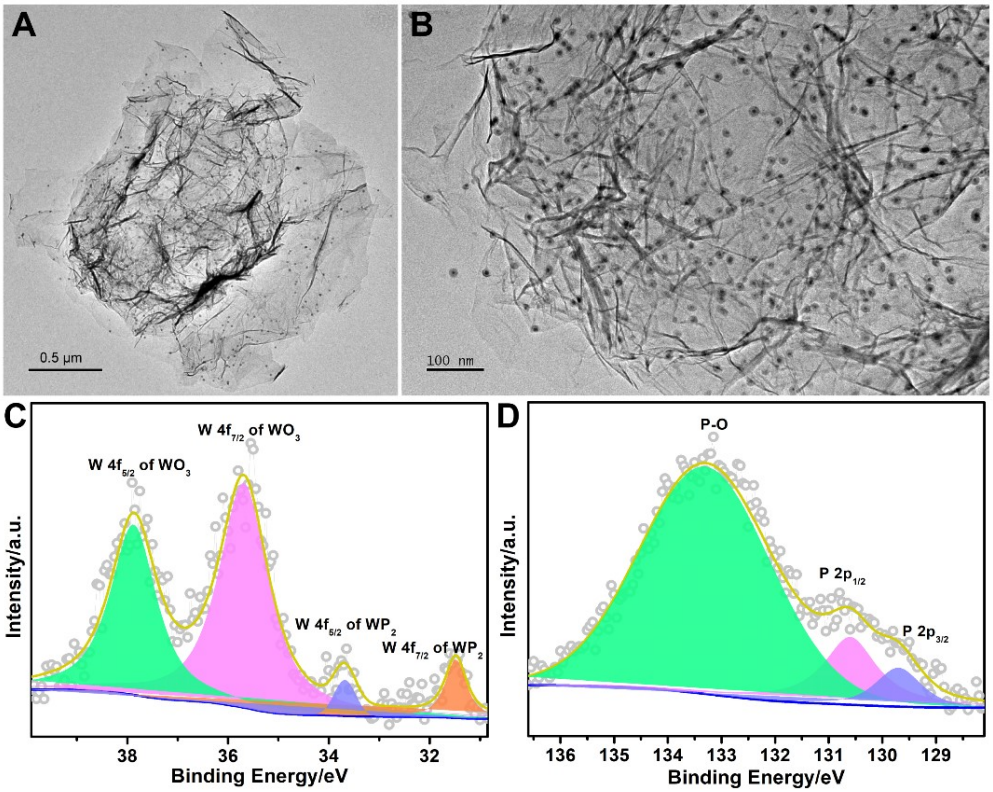

Fig. S7 TEM image and high-resolution W 4f (**B**) and P 2p (**C**) XPS spectra of WP_2/G.

Table S1 Detailed comparison of the performance of G@W-Co-P in 0.5 M H_2SO_4 with those of representative non-noble-metal HER catalysts.

Catalyst	Loading (mg cm^{-2})	j_0 (mA/cm^{-2})	Onset overpotential (mV)	η_{10} (mV)	Tafel slope (mV dec^{-1})	Ref.
FeP_2/C NPs	0.425	0.00175		220	66	S1
CoP NFs	0.265			122	54.8	S2
W-W_2C/CNT-6	0.28			155	56	S3
Fe doped NiS_2				198	42	S4
MoPS/NC	0.56		23	92	56	S5
CoP/CNT	0.285	0.13	40	122	54	S6
N,P-MoxC NF	0.265			107	65.1	S7
CoP/NCNHP				140	53	S8
CoP@NG	0.283			158	63.8	S9
Mo_2C-N-CNFs	0.255	0.0473		167	70	S10
Ni_2P/CNT	0.2	0.0537		124	53	S11
WP_2 nanorods	0.285	0.013	101	148	52	S12
FeP GS	0.28	0.12	30	123	50	S13
Ni_2P@NPCNFs	0.56			63.2	56.7	S14
MoP@PC	0.41			153	66	S15
CoP/Co_2P@NC-2				126	79	S16
FeP NPs@NPC	1.4	0.126		130	67	S17
CoP-OMC	0.285	0.161	77.74	112.18	56.67	S18
α-MoC_{1-x}/NC				142	74	S19
CoP-N-C	0.425	0.16	31	91	42	S20
Ni_2P hollow NPs	1	0.033		117	46	S21
G@W-Co-P	0.5	0.128	13	91.5	40.7	This work

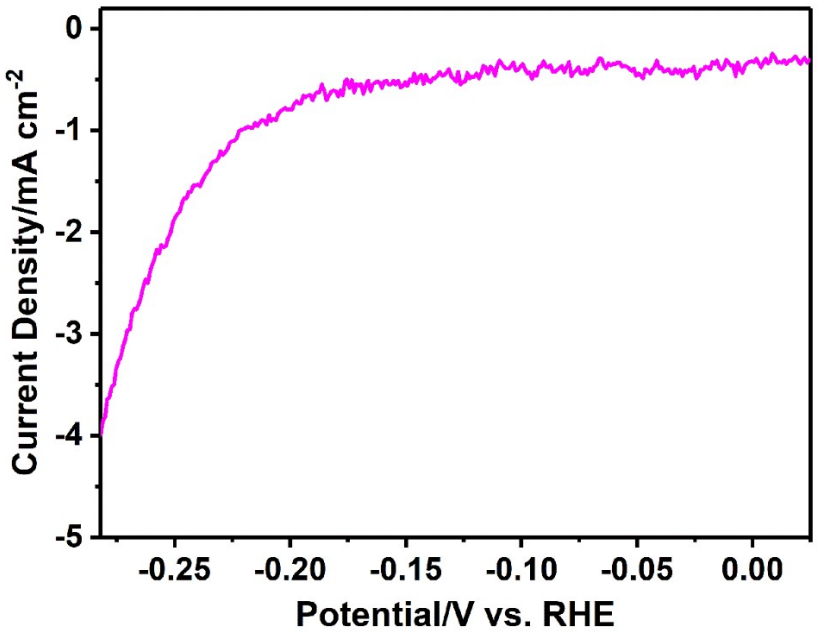

Fig. S8 Enlarged LSV curve of WP_2/G in 0.5 M H_2SO_4.

Table S2 Detailed comparison of the performance of G@W-Co-P in 1 M KOH with those of representative non-noble-metal HER catalysts.

Catalyst	Loading (mg cm^{-2})	Onset overpotential (mV)	η_{10} (mV)	Tafel slope (mV dec^{-1})	Ref.
CoP NFs	0.265		136	56.2	S1
CoTeNR/NF	1.3		202	115	S22
Co_3O_4/MoS_2	2		205	98	S23
CoP/CC	0.92	45	106	93	S24
NiCoP/NPC HFSs	0.2	~80	128	70	S25
CoP/rGO-400	0.285		150	38	S26
$Cu_{0.3}Co_{0.27}P$/NC	0.4		220	112	S27
CoP/NCNHP			115	66	S8
CoP@NG	0.283		182	59.6	S9
NiCoP/CNF900		100	130	83	S28

Co-PNCNFs	0.56		249	92	S29
$Ni_{0.69}Co_{0.35}P$	3.5		167	47	S30
$Ni_{12}P_5$/NF	3		170	106	S31
FeP NAs/CC	1.5	86	218	146	S32
W-W2C/CNT-6	0.28		147	51	S3
Co_4Ni_1P NTs	0.19		129	52	S33
CoFe/NF			110	35	S34
NiCoP@NF			155	115	S35
WP_2 nanorods		149	225	84	S12
EG/H-Co0.85Se|P	2.1		150	83	S36
NiCoP/rGO	0.19		209	124.1	S37
G@W-Co-P	0.5	16.1	102.3	61.2	This work

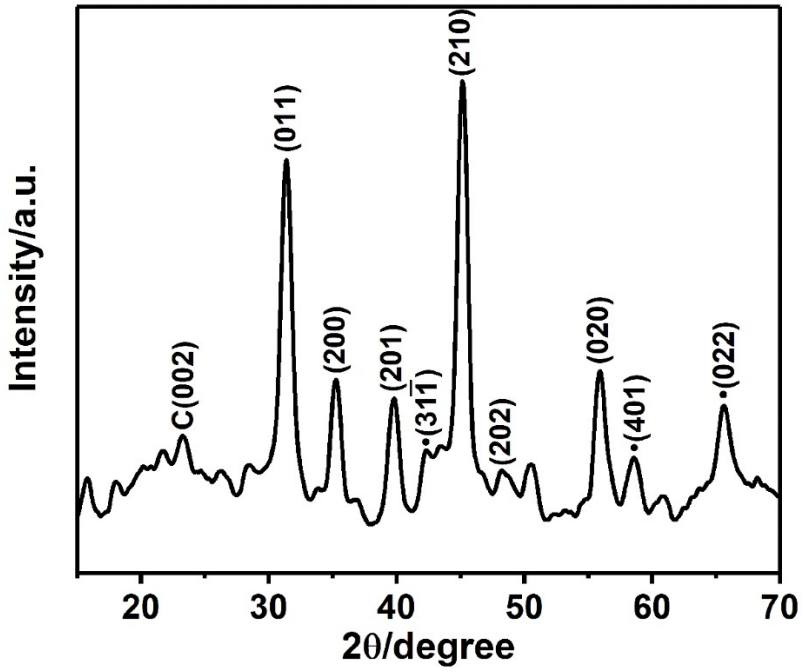

Fig. S9 XRD pattern of G@Co-W-P after the durability tests.

References

[S1] J. Jiang, C. Wang, J. Zhang, W. Wang, X. Zhou, B. Pan, K. Tang, J. Zuo, Q. Yang, *J. Mater. Chem. A* 2015, **3**, 499-503.

[S2] L. Ji, J. Wang, X. Teng, T. J. Meyer, Z. Chen, *ACS Catal.* 2020, **10**, 412-419.

[S3] Y. Hu, B. Yu, M. Ramadoss, W. Li, D. Yang, B. Wang, W. Chen, *ACS Sustain. Chem. Eng.* 2019, **7**, 10016-10024.

[S4] T. Wang, X. Guo, J. Zhang, W. Xiao, P. Xi, S. Peng, D. Gao, *J. Mater. Chem. A* 2019, **7**, 4971-4976.

[S5] Y. Huang, X. Song, J. Deng, C. Zha, W. Huang, Y. Wu, Y. Li, *Appl. Catal. B: Environ.* 2019, **245**, 656-661.

[S6] Q. Liu, J. Tian, W. Cui, P. Jiang, N. Cheng, A. M. Asiri, X. Sun, *Angew. Chem. Int. Edit.* 2014, **53**, 6710-6714.

[S7] L. Ji, J. Wang, X. Teng, H. Dong, X. He, Z. Chen, *ACS Appl. Mater. Interfaces* 2018, **10**, 14632-14640.

[S8] Y. Pan, K. Sun, S. Liu, X. Cao, K. Wu, W. C. Cheong, Z. Chen, Y. Wang, Y. Li, Y. Liu, D. Wang, Q. Peng, C. Chen, Y. Li, *J. Am. Chem. Soc.* 2018, **140**, 2610-2618.

[S9] Y. Lu, W. Hou, D. Yang, Y. Chen, *Electrochim. Acta* 2019, **307**, 543-552.

[S10] Z. Y. Wu, B. C. Hu, P. Wu, H. W. Liang, Z. L. Yu, Y. Lin, Y. R. Zheng, Z. Li, S. H. Yu, *NPG Asia Mater.* 2016, **8**, e288.

[S11] Y. Pan, W. Hu, D. Liu, Y. Liu, C. Liu, *J. Mater. Chem. A* 2015, **3**, 13087-13094.

[S12] H. Du, S. Gu, R. Liu, C. M. Li, *J. Power Sources* 2015, **278**, 540-545.

[S13] Z. Zhang, B. Lu, J. Hao, W. Yang, J. Tang, *Chem. Commun.* 2014, **50**, 11554-11557.

[S14] M. Q. Wang, C. Ye, H. Liu, M. Xu, S. J. Bao, *Angew. Chem. Int. Edit.* 2018, **57**, 1963-1967.

[S15] J. Yang, F. Zhang, X. Wang, D. He, G. Wu, Q. Yang, X. Hong, Y. Wu, Y. Li, *Angew. Chem. Int. Edit.* 2016, **55**, 12854-12858.

[S16] X. Lv, J. Ren, Y. Wang, Y. Liu, Z. Y. Yuan, *ACS Sustain. Chem. Eng.* 2019, **7**, 8993-9001.

[S17] Z. Pu, I. S. Amiinu, C. Zhang, M. Wang, Z. Kou, S. Mu, *Nanoscale* 2017, **9**, 3555-3560 .

[S18] M. Li, X. Liu, Y. Xiong, X. Bo, Y. Zhang, C. Han, L. Guo, *J. Mater. Chem. A* 2015, **3**, 4255-4265.

[S19] L. Lin, Z. Sun, M. Yuan, H. Yang, H. Li, C. Nan, H. Jiang, S. Ge, G. Sun, *ACS Sustain.*

Chem. Eng. 2019, **7**, 9637-9645.

[S20] Z. Zhang, J. Hao, W. Yang, J. Tang, *ChemCatChem* 2015, **7**, 1920-1925.

[S21] E. J. Popczun, J. R. McKone, C. G. Read, A. J. Biacchi, A. M. Wiltrout, N. S. Lewis, R. E. Schaak, *J. Am. Chem. Soc.* 2013, **135**, 9267-9270.

[S22] L. Yang, H. Xu, H. Liu, D. Cheng, D. Cao, *Small Methods* 2019, **3**, 1900113.

[S23] A. Muthurasu, V. Maruthapandian, H. Y. Kim, *Appl. Catal. B: Environ.* 2019, **248**, 202-210.

[S24] J. Tian, Q. Liu, A. M. Asiri, X. Sun, *J. Am. Chem. Soc.* 2014, **136**, 7587-7590.

[S25] M. Yi, B. Lu, X. Zhang, Y. Tan, Z. Zhu, Z. Pan, J. Zhang, *Appl. Catal. B: Environ.* 2021, **283***,* 119635.

[S26] L. Jiao, Y. X. Zhou, H. L. Jiang, *Chem. Sci.* 2016, **7**, 1690-1695.

[S27] J. Song, C. Zhu, B. Z. Xu, S. Fu, M. H. Engelhard, R. Ye, D. Du, S. P. Beckman, Y. Lin, *Adv. Energy Mater.* 2017, **7**, 1601555.

[S28] S. Surendran, S. Shanmugapriya, A. Sivanantham, S. Shanmugam, R. K. Selvan, *Adv. Energy Mater.* 2018, **8**, 1800555.

[S29] Y. Zhao, J. Zhang, K. Li, Z. Ao, C. Wang, H. Liu, K. Sun, G. Wang, *J. Mater. Chem. A* 2016, **4**, 12818-12824.

[S30] Z. Yin, C. Zhu, C. Li, S. Zhang, X. Zhang, Y. Chen, *Nanoscale* 2016, **8**, 19129-19138.

[S31] P. W. Menezes, A. Indra, C. Das, C. Walter, C. Goebel, V. Gutkin, D. Schmeisser, M. Driess, *ACS Catal.* 2017, **7**, 103-109.

[S32] Y. Liang, Q. Liu, A. M. Asiri, X. Sun, Y. Luo, *ACS Catal.* 2014, **4**, 4065-4069.

[S33] L. Yan, L. Cao, P. Dai, X. Gu, D. Liu, L. Li, Y. Wang, X. Zhao, *Adv. Funct. Mater.* 2017, **27**, 1703455.

[S34] P. Babar, A. Lokhande, H. H. Shin, B. Pawar, M. G. Gang, S. Pawar, J. M. Kim, *Small* 2018, **14**, 1702568.

[S35] A. Han, H. Chen, H. Zhang, Z. Sun, P. Du, *J. Mater. Chem. A* 2016, **4**, 10195-10202.

[S36] Y. Hou, M. Qiu, T. Zhang, X. Zhuang, C. S. Kim, C. Yuan, X. Feng, *Adv. Mater.* 2017, **29**, 1701589.

[S37] J. Li, M. Yan, X. Zhou, Z. Q. Huang, Z. Xia, C. R. Chang, Y. Ma, Y. Qu, *Adv. Funct. Mater.* 2016, **26**, 6785-6796.